

HOSTED BY

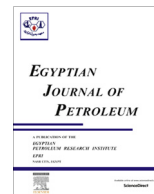


ELSEVIER

Contents lists available at ScienceDirect

Egyptian Journal of Petroleum

journal homepage: www.sciencedirect.com



Full Length Article

Reservoir characterization utilizing the well logging analysis of Abu Madi Formation, Nile Delta, Egypt

M. Mahmoud^a, M. Ghorab^b, T. Shazly^b, A. Shibl^a, Abeer A. Abuhagaza^{b,*}^a Ain Shams University, Egypt^b Egyptian Petroleum Research Institute, Egypt

ARTICLE INFO

Article history:

Received 24 October 2016

Revised 8 November 2016

Accepted 13 November 2016

Available online xxxx

Keywords:

Reservoir characterization

Late Miocene

Abu Madi Formation

Well logging

Abu Madi/El Qar'a fields

ABSTRACT

The petrophysical evaluation of the Late Miocene Abu Madi Formation were accomplished based on the open hole logs of eighteen wells in Abu Madi–El Qar'a gas fields, onshore Nile Delta, Egypt. The lithological contents of this rock unit were analyzed using the cross plots of petrophysical parameters including shale volume, porosity and hydrocarbon saturation. The neutron /density cross-plots, M-N and RHOMAA–DTMAA and litho-saturation cross plots of the studied wells show that the main lithology of the lower part of Abu Madi Formation is calcareous sandstones with shale intercalations in most of the studied wells while its lithology is mainly shale with sand intercalations in wells AM-13, AM-21 and AM-7. The lithology of the upper part of Abu Madi Formation in most wells is composed mainly of shale while its lithology in AM-13, AM-21 and AM-7 wells is composed of sandstone with shale intercalations. The thorium-potassium cross plots indicate that, Abu Madi Formation was deposited mostly in fluvial to shallow marine environments according to the presence of mica and illite in the southern area and montmorillonite at the northern area as dominant clay minerals. Contour maps of several petrophysical parameters such as effective thickness, average shale volume, average porosity and hydrocarbon saturation showed that both lower and upper parts of Abu Madi Formation in the study area have promising reservoirs characteristics; in which the prospective area for gas accumulation located toward the central part.

Crown Copyright © 2016 Production and hosting by Elsevier B.V. on behalf of Egyptian Petroleum Research Institute. This is an open access article under the CC BY-NC-ND license (<http://creativecommons.org/licenses/by-nc-nd/4.0/>).

1. Introduction

The Nile Delta is situated near to the northeastern margin of the African plate and forms part of the Eastern Mediterranean basin. The Nile Delta is a giant gas province that has attracted attention due to its approximately 42 TCF of proven reserves and approximately 50 TCF of undiscovered potential. Following the first commercial discovery in 1966 when the Abu Madi-1 well proved the production potential of the Messinian Abu Madi sandstones [1], exploration on the onshore Delta has focused on Oligocene/Early Miocene through Pleistocene clastic reservoirs. The study is focused on the Abu Madi and El Qar'a gas fields, these fields are the giant gas fields located in the northern part of the Nile Delta; southeast of Lake Burullus about 200 km north of Cairo city (Fig. 1). El Qar'a Gas field was considered by [2] as an extension

to the north of Abu Madi Field. In which the main target is the Late Messinian Abu Madi Formation [3]. This study involves lithology analysis of Abu Madi Formation based on logging parameter cross-plot by using logging data of 18 gas wells, and evaluation of petrophysical parameters such as shale content, porosity, water and hydrocarbon saturation.

2. Geological setting

The Nile Delta lies on unstable shelf characterized by thick sedimentary section covering the high basement relief due to block faulting. [4] showed that the North Nile Delta basin is structurally controlled by three main fault trends; 1 – NW–SE fault trend, 2 – NE–SW fault trend and 3 – E–W fault trend. The interplay of these fault trends builds up the overall tectonic framework of north Nile Delta basin (Fig. 2).

The sedimentary section in the Nile Delta area with gas potentiality seems to be limited to the Neogene formations trapped against listric faults or draped over tilted fault blocks. However

Peer review under responsibility of Egyptian Petroleum Research Institute.

* Corresponding author.

E-mail address: aaa_geo107@yahoo.com (A.A. Abuhagaza).<http://dx.doi.org/10.1016/j.ejpe.2016.11.003>

1110-0621/Crown Copyright © 2016 Production and hosting by Elsevier B.V. on behalf of Egyptian Petroleum Research Institute.

This is an open access article under the CC BY-NC-ND license (<http://creativecommons.org/licenses/by-nc-nd/4.0/>).

Please cite this article in press as: M. Mahmoud et al., Reservoir characterization utilizing the well logging analysis of Abu Madi Formation, Nile Delta, Egypt, *Egypt. J. Petrol.* (2016), <http://dx.doi.org/10.1016/j.ejpe.2016.11.003>

few wells which are mostly located in the south delta block. The sedimentary rocks penetrated in Abu Madi/El Qar'a fields consist of thick clastics representing Miocene-Holocene time interval. These rocks were described by [5,6]. The studied section is differentiated into the rock units: Qantara, Sidi Salem, Qawasim, and Abu Madi formations of the Miocene age; Kafr El Sheikh and El Wastani formations of the Pliocene age; Mit Ghamr Formation of late Pliocene-Pleistocene age and the Bilqas Formation of recent age. All these formations consist essentially of clastic sediments (shale, sand, and silt).

3. Materials and methods

The hydrocarbon saturation of Abu Madi reservoirs in the studied area was evaluated in eighteen wells from south to north (AM-13, AM-12, AM-16, AM-21, AM-17, AM-14, AM-7, AM-19, AM-11ST, AM-11, AM-8, AM-15, EQ-2, EQ-3, EQ-5, EQ-6, EQ-9, and EQN-1). The basis for reservoir oil and gas potentiality evaluation is the petrophysical analysis of drilled targets in all the wells, including the vertical distribution of petrophysical parameters, lithology interpretation from parameters cross plots and lateral distribution changes of various parameters. The available 1og data for the studied units in all the wells were quality control inspected, including deep and shallow laterologs (LLD, ILD, LLS, LLM and MSFL), neutron porosity, bulk density, acoustic and gamma ray. The borehole environmental corrections and interpretation were carried out using Schlumberger software TECHLOG (2011.2.1). The lithology components of Abu Madi Formation in all wells were investigated by using crossplots of logging parameters (including dia-porosity density-neutron cross-plots, and tri-porosity M-N and rhomaa-dtmaa crossplot), the results from different crossplots are slightly different according to the properties of each parameter.

Shale content (Vsh) may be evaluated using a variety of petrophysical indexes, such as gamma-ray, neutron porosity, resistivity and neutron porosity/density as a double curve clay indicator [7]. In the present study the corrected porosity was estimated using a combination of the density and neutron logs [8]. The effective water saturation (Sw) in clean and shaly zones was computed using the Indonesia [9]. Determination of the hydrocarbon saturation (Sh) and discrimination of hydrocarbons into the different types of gas or oil are performed.

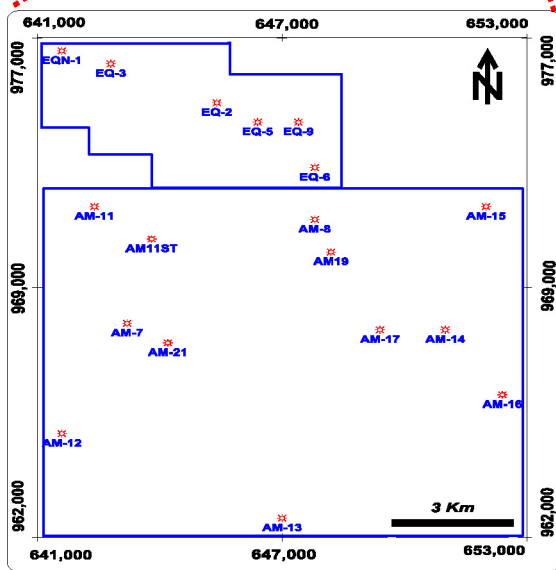


Fig. 1. Location map of the study area.

Pre-Miocene formations of the base of this Neogene sequence may also be considered as future exploration plays. Mesozoic reservoirs are present at greater depth and have been only penetrated by a

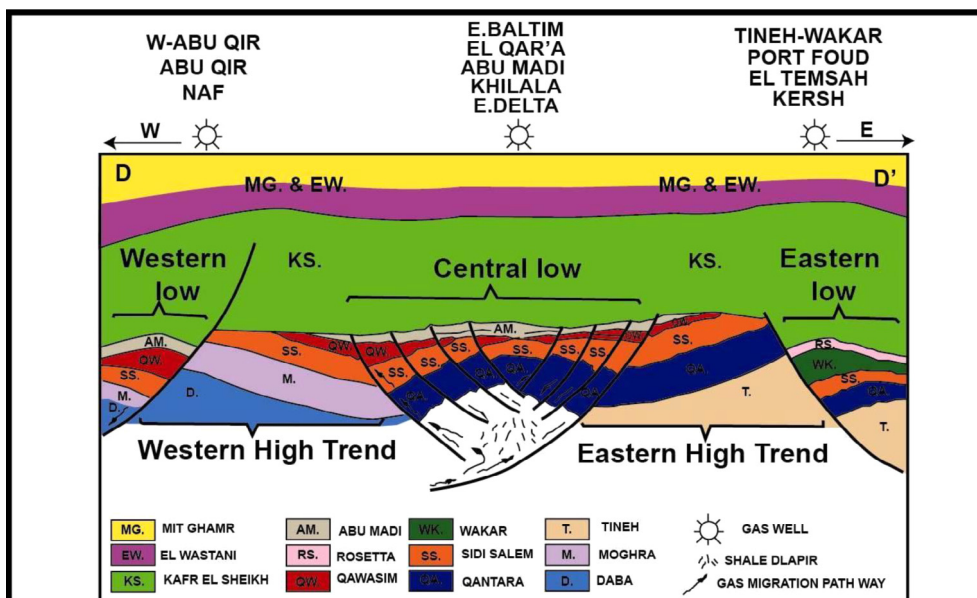


Fig. 2. Geological model of the North Nile Delta block after [4].

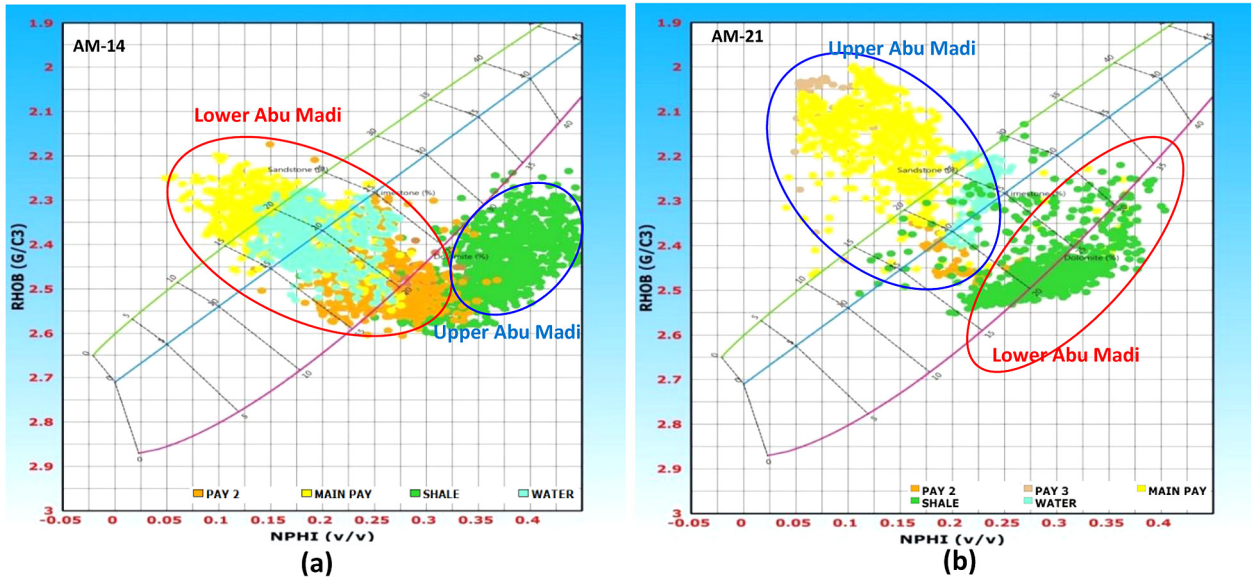


Fig. 3. RHOB-NPHI cross-plot of (a) AM-14 and (b) AM-21wells.

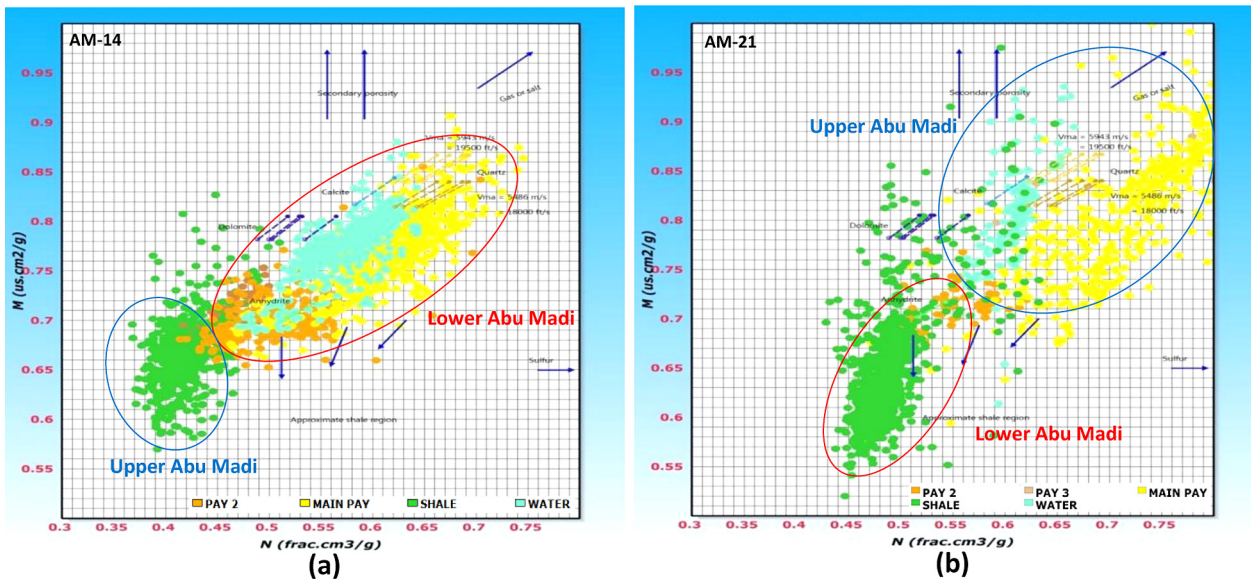


Fig. 4. M-N cross-plot of (a) AM-14 and (b) AM-21wells.

4. Result and discussion

4.1. Lithological interpretation using cross-plots

The lithological contents of Abu Madi Formation were investigated using the combination of different logs cross-plot such as the dia-porosity density–neutron cross-plots, thorium–potassium cross-plots and tri-porosity M-N and RHOMAA–DTMA in the studied wells. Abu Madi Formation in the studied wells was subdivided lithologically into lower and upper parts of Abu Madi Formation and also divided petrophysically into six zones, main pay, pay2, pay3, pay4, water and the green color shale and shaly zones according to the average of shale and hydrocarbon saturation in each zone.

4.1.1. Neutron (NPHI) vs. density (RHOB) cross-plot

The dia-porosity RHOB – NPHI cross-plot shows that the data points of the Lower Abu Madi unit (represented by main pay, pay 2 and water zones in most of the wells, AM-14 an example) (Fig. 3a) are concentrated on sandstone line and some points are directed towards the limestone line that reflected the presence of calcareous materials. The main lithology of the lower part of Abu Madi Formation is composed mainly of sandstone and shale intercalations in all wells except AM-13, AM-21 and AM-7 wells becomes more shaly (Fig. 3b). In contrast, the lithology of the upper part of Abu Madi Formation is composed mainly of shale with few sandstone intercalations in all wells except AM-13, AM-21 and AM-7 wells in which this part becomes more sandy (Fig. 3b). The majority points of main pay zone in both lower and upper parts of Abu

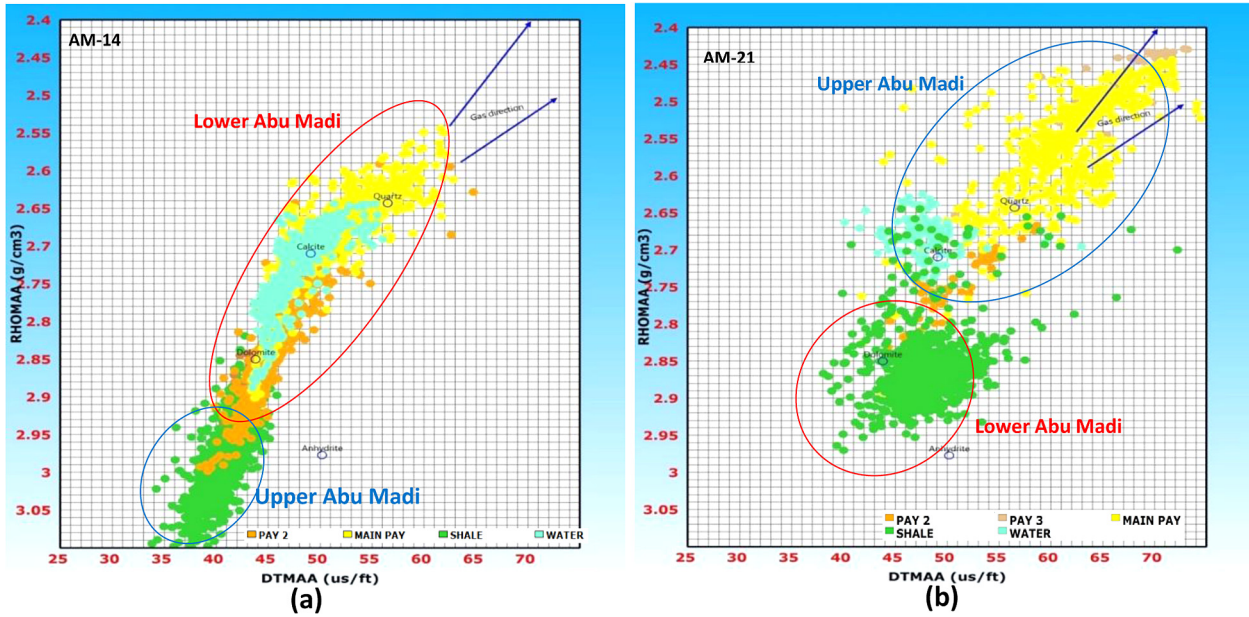


Fig. 5. RHOMAA–DTMAA cross-plot of (a) AM-14 and (b) AM-21 wells.

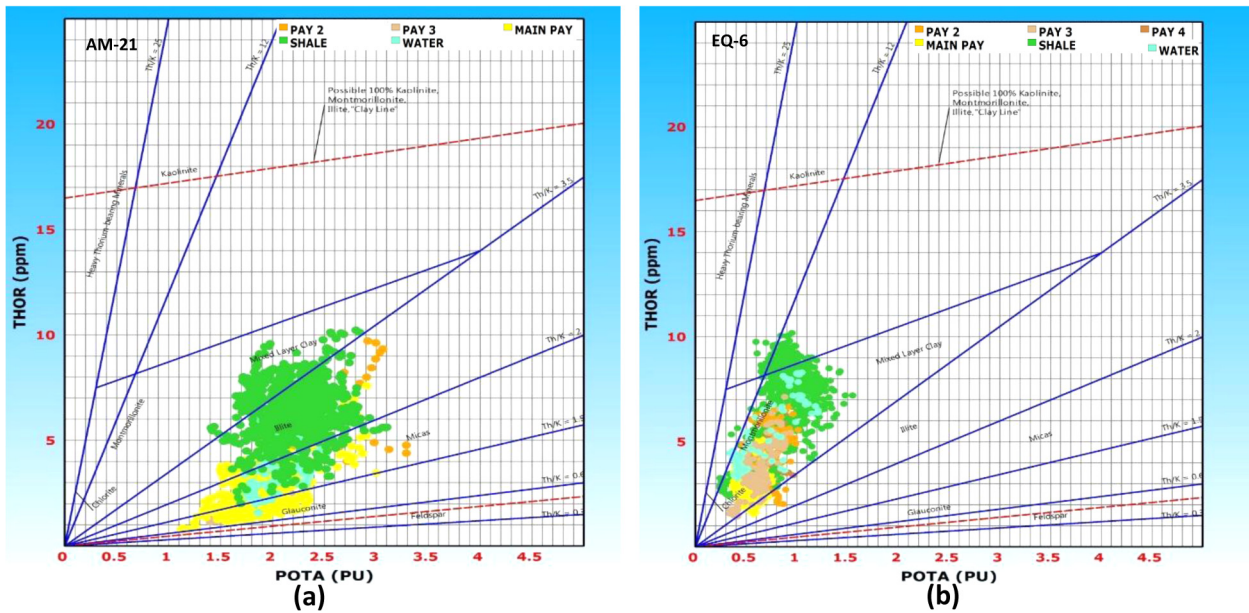


Fig. 6. Thorium–Potassium cross-plot of (a) AM-21 and (b) EQ-6 wells.

Madi Formation shifted to the north western direction due to the effect of gas.

4.1.2. Tri-porosity M–N and RHOMAA–DTMAA cross-plots

By comparison, the tri-porosity M–N and RHOMAA–DTMAA cross-plots (Figs. 4 and 5a, b) and the dia-porosity NPHI/RHOB cross-plot are consistent; the data points are concentrated at the quartz point and some points are shifted toward calcite region indicated the presence of calcareous minerals, the data points migrated toward the north western region indicating the effect of gas, this description showing the main lithology of the lower part of Abu Madi Formation is sandstone with occasional shale intercalations in all wells except AM-13, AM-21 and AM-7 wells where

the data points grouped around the shale area indicating more shaly formations.

On the other hand, the upper part of Abu Madi Formation exhibits high shale content in all wells except AM-13, AM-21 and AM-7 wells becomes more sandy that is in agreement with the results from neutron-density crossplots.

4.1.3. Thorium–potassium cross-plots

Thorium–potassium crossplot of Abu Madi Formation for AM-21 and EQ-1 wells as example (Fig. 6) is showing that the dominant clay minerals are mica and illite at the southern area and montmorillonite at the northern part of the studied area which reflect the fluvial to shallow marine environment of deposition of Abu Madi Formation.

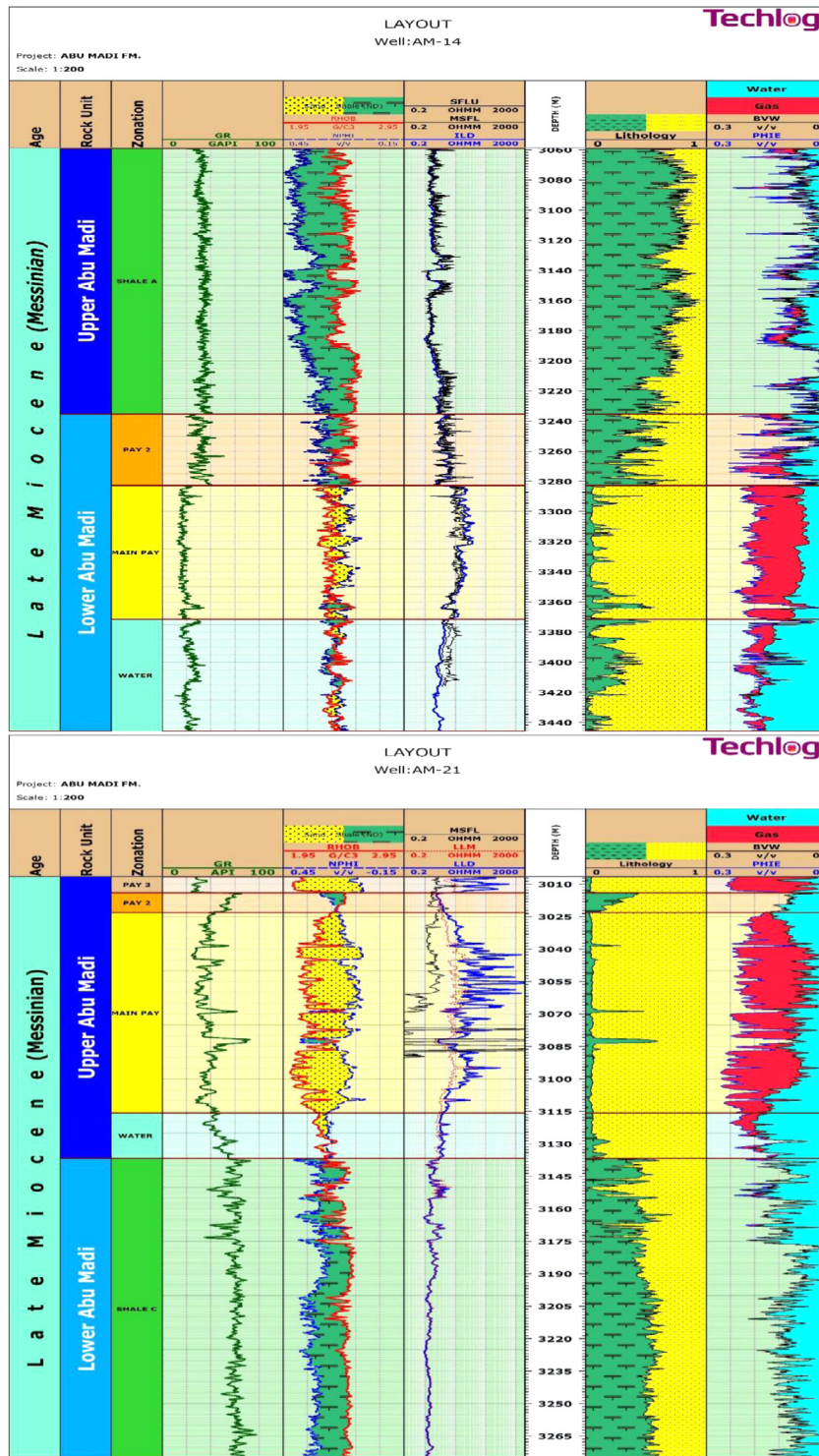


Fig. 7. Litho-saturation crossplot for AM-14 and AM-21 wells (as an example of Lower and Upper Abu Madi reservoirs) in Abu Madi gas field.

4.1.4. Lithology-saturation cross-plot

The vertical distribution in the form of litho-saturation cross-plots shows the vertical variation of lithology, water saturation and gas content for each zone of Abu Madi Formation using different water saturation models for clean and shaly sand reservoirs. Density, neutron porosity and resistivity were adopted to evaluate various reservoir intervals.

The cross plots of all the examined intervals from the studied wells have been constructed in the present work as examples of AM-14 and AM-21 wells (Fig. 7), shows that the lower part of

Abu Madi Formation is all sandstone with shale intercalation in all the studied wells; except AM-13, AM-21 and AM-7 wells that have more shale. The upper part of Abu Madi Formation is made up of shale and small amount of sandstone in all wells but only AM-13, AM-21 and AM-7 wells have more sand than the lower part. AM-12, AM-15 and AM-11 wells have high shale content in both lower and upper parts of Abu Madi Formation.

The lithologic cross section (Fig. 8 as an example) shows that the thickness of the lower part of Abu Madi Formation which is considered the main reservoir in most of the studied wells increase

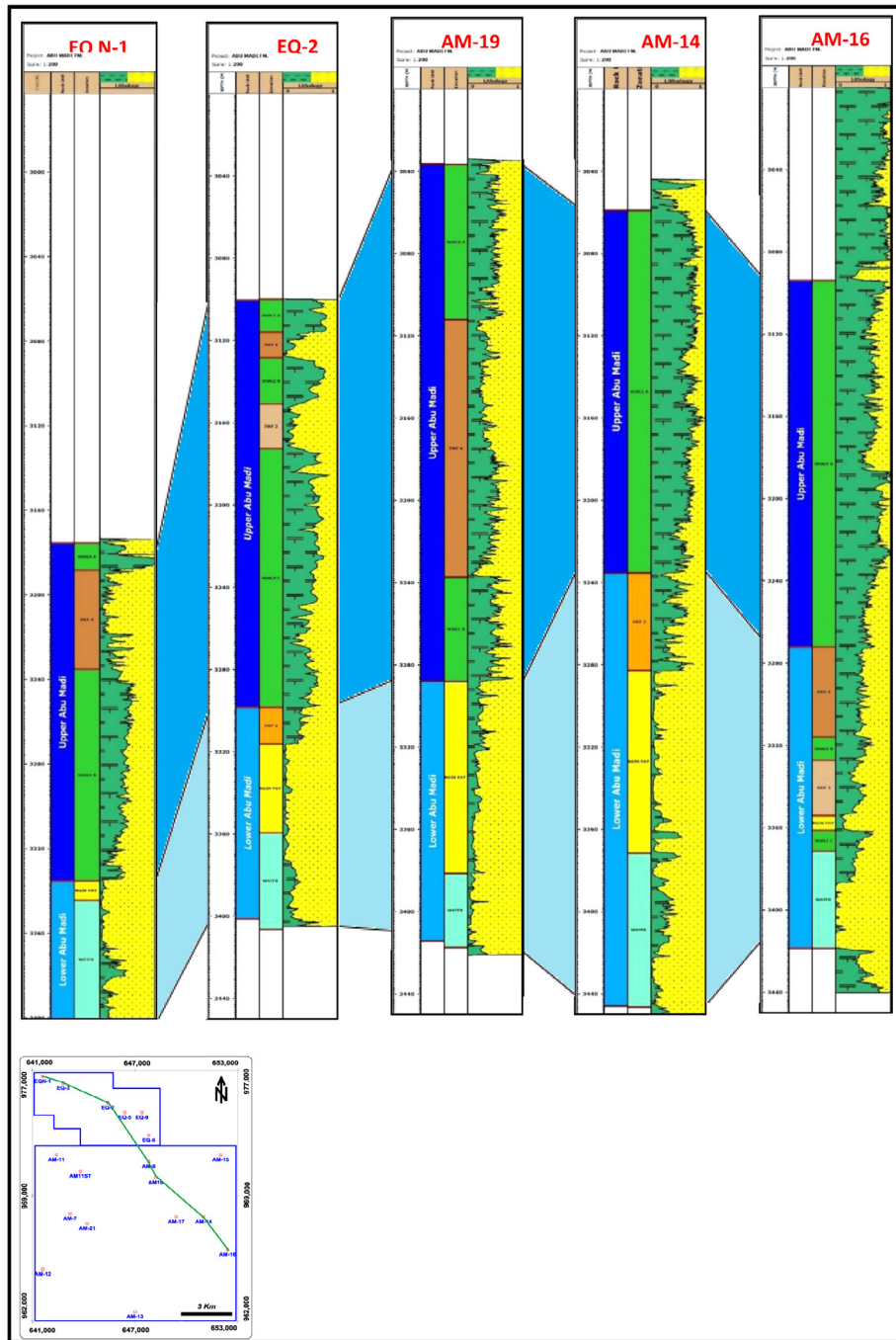


Fig. 8. The lithologic profile of EQN-1, EQ-2, AM-19, AM-14 and AM-16 wells.

toward the central east area in AM-14 and EQ-2 wells and the gamma ray reading increase toward the right and left sides of the study area due to an increase of shale interbeds in AM-16 and EQN-1 wells.

4.2. Formation evaluation

The reservoir parameters of Abu Madi Formation (main pay, pay 2 pay 3 and pay 4 zones) extracted from well logging data were averaged and shown in (Table 1). Contour maps for these parameters (weighted average values) were prepared using Golden Software Surfer v.8 to reflect the lateral distribution throughout the Lower and Upper Abu Madi reservoirs. The maps are of two types;

the first one is for the main pay only and the second type of maps is the total average of all studied zones (main pay, pay 2 pay 3 and pay 4 zones).

4.2.1. Net thickness distribution map

The net thickness distribution map is constructed to discuss the horizontal variation of thinning and thickening of the studied rock units. The net thickness of sandstone in the Lower and Upper Abu Madi reservoirs concentrated in the main pay zone in which its thickness increases toward the central part of the studied wells from south to north and ranged from 34.64 m at AM-13 well (Upper part of Abu Madi Formation) to 87 m at EQ-9 well (Lower part of Abu Madi Formation). The thickness of the main pay in

Table 1
Reservoir parameters of Abu Madi Formation.

Well	Formation part	Zonation	Top	Bottom	Net Thickness	Av_VSH	Av_PHIE	Av_Sh
AM-13	Upper Abu Madi	PAY 4	3026	3038	12	7.9	23.6	54
		PAY 2	3077	3096	19	23.1	19.6	58
		MAIN PAY	3096	3131	35	3	22	77
		Average			66	11.3	21.83	63
AM-12	Lower Abu Madi	PAY 4	3335	3385	50.37	32.1	11.5	16.6
		PAY 4	3272	3316	43.68	32.7	6.8	44.5
		PAY 3	3327	3354	26.93	11.6	12.2	52.5
		MAIN PAY	3354	3361	7	8.6	17	59
AM-16		Average			77.6	17.6	12	52
		PAY 3	3007	3014	7.5	3.4	22.7	70.9
		PAY 2	3014	3023	9.17	40.5	10.1	16.6
		MAIN PAY	3023	3116	93	7	20.5	51
AM-21	Upper Abu Madi	Average			109.27	18.77	17.77	49.03
		PAY 2	3211	3283	72.25	36.8	9.8	23.4
		MAIN PAY	3283	3372	89	5.7	18.3	62.2
		Average			161.3	21.25	14.05	42.8
AM-14	Lower Abu Madi	PAY 4	3130	3146	15	64	7.1	29
		PAY 3	3307	3317	10	15.1	15	45.6
		MAIN PAY	3328	3363	35	4.2	18.5	56.3
		Average			60	27.8	12.77	43.63
AM-17	Upper Abu Mad	PAY 4	3028	3052	23.68	10.4	16.5	70.4
		PAY 4	3052	3122	69.99	20.1	15.5	38.7
		PAY 2	3277	3321	43.81	3.4	11.3	40.4
		Average			137.5	11.3	14.43	49.83
AM-7	Lower Abu Madi	PAY 4	3103	3183	80.26	33.7	16.2	47.9
		PAY 3	3226	3238	11.95	23.1	17.5	42.9
		PAY 2	3288	3352	63.94	18.7	16.7	58.7
		MAIN PAY	3352	3375	23	2.2	24	45
AM-19	Lower Abu Madi	Average			179.2	19.4	16.1	48.6
		PAY 4	3226	3234	10.66	16	14.3	32.1
		PAY 3	3241	3247	7.49	7.5	16.6	34.6
		PAY 2	3247	3250	3.97	26.2	11	26.1
AM11-ST		MAIN PAY	3250	3268	23.78	2.4	22.7	44
		Average			45.9	13.03	16.15	34.2
		PAY 4	3081	3158	76.25	36.5	12.6	32.2
		PAY 3	3213	3220	7.23	17.5	16	27.8
AM-8	Lower Abu Madi	PAY 2	3261	3272	11.47	24.1	14.9	39.9
		MAIN PAY	3272	3331	58	3.2	19	52
		Average			153	20.3	15.6	38
		PAY 4	3160	3200	40.62	15.9	24.4	22.1
AM-11	Upper Abu Madi	PAY 2	3461	3463	1.11	6.1	25.5	17.7
		Average			41.73	11	24.95	19.9
		PAY 4	3208	3258	50.35	13.6	19.4	32.1
AM-15	Lower Abu Madi	PAY 4	3208	3258	50.35	13.6	19.4	32.1
		PAY 4	3076	3191	114.87	48.8	11.8	34.2
EQ-6	Upper Abu Madi	PAY 2	3201	3288	87.37	35.1	13.2	31.7
		MAIN PAY	3288	3340	52	4.1	18	40
		Average			254.2	29.3	11	35.3
		PAY 4	3113	3121	10.24	25.4	21.5	34.8
EQ-9	Upper Abu Madi	PAY 3	3146	3166	22.11	4	21.4	24.2
		PAY 2	3248	3261	26.88	24.7	15.1	48.9
		MAIN PAY	3314	3401	87	4	16.4	39
		Average			146.23	14.5	18.6	36.7
EQ-5	Lower Abu Madi	PAY 4	3141	3173	32.24	11.6	17.2	26.4
		PAY 2	3239	3294	55.3	26.7	12.6	24.8
		MAIN PAY	3294	3354	59	2.4	23.3	44
		Average			146.5	13.57	17.7	31.7
EQ-2	Upper Abu Madi	PAY 4	3116	3128	12.41	26	18	22.8
		PAY 3	3151	3173	21.68	11.7	17.6	18.3
		PAY 2	3299	3316	17.73	28.9	15.2	51.3
		MAIN PAY	3316	3359	43	3	20.9	38
EQ-3	Lower Abu Madi	Average			94.8	17.4	17.9	32.6
		PAY 4	3184	3233	48.54	14.4	16.4	30.1
		PAY 2	3326	3357	31.06	45.1	10.3	39.3
		MAIN PAY	3357	3372	15	5.9	14.8	40
EQ N-1	Upper Abu Madi	Average			94.6	21.8	13.83	36.5
		PAY 4	3232	3280	48	44	16	35
		MAIN PAY	3383	3392	9	7	16	33
EQ N-1	Lower Abu Madi	Average			57	25.5	16	34

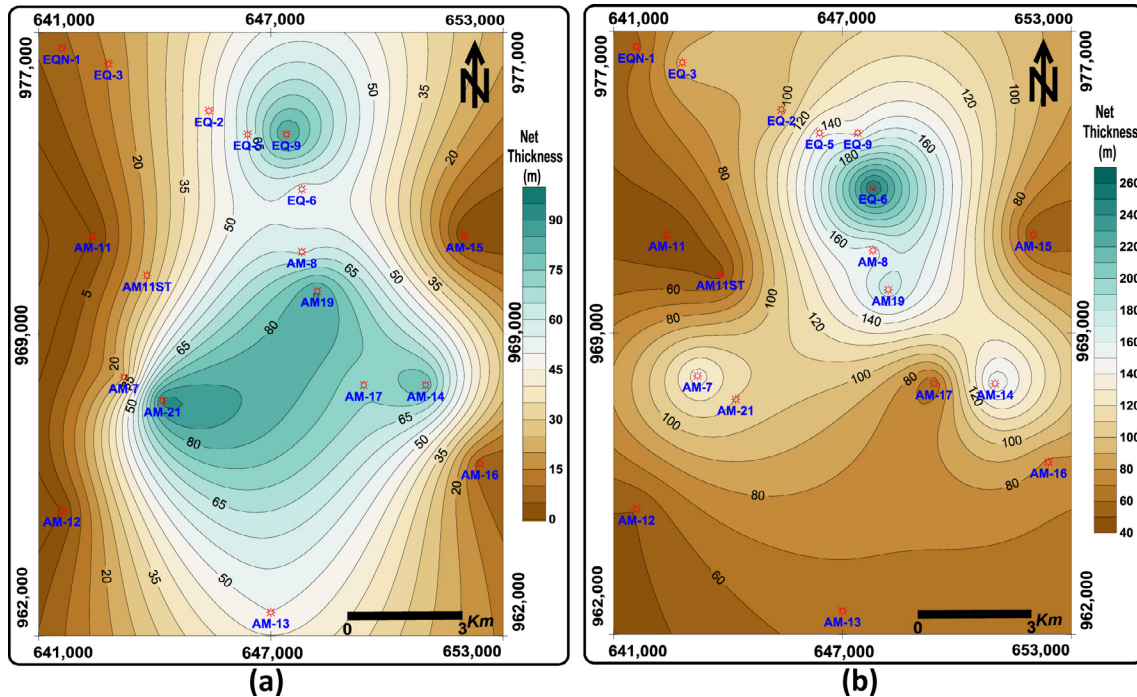


Fig. 9. The net thickness distribution map of (a) main pay zone and (b) total pay zones.

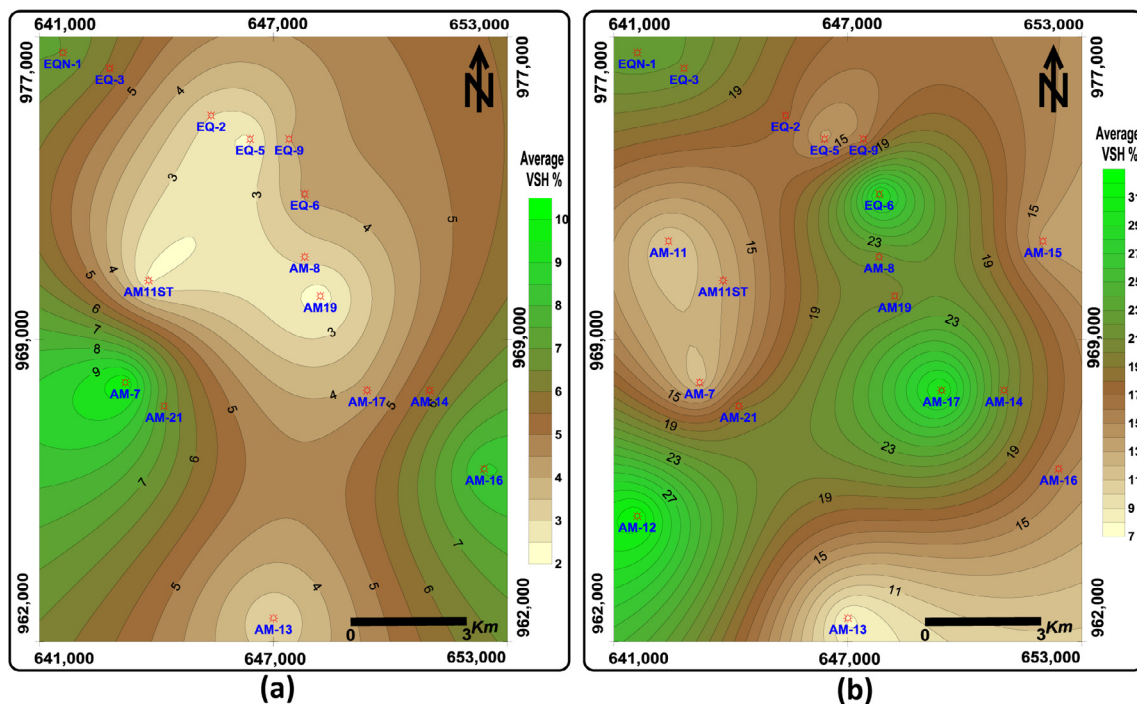


Fig. 10. The average shale content distribution map of (a) main pay zone and (b) total pay zones.

Abu Madi Formation decreases in both right and left sides of the studied area and absent in AM-12, AM-11, AM-5 and AM-15 wells. (Fig. 9a, b). The net thickness of all pay zones shows that the minimum thickness is 41.73 m in the western side of the studied area at AM-11 well and the maximum thickness is 254.44 m at EQ-6 well in the middle area (Fig. 9b). Consequently, the best locations for drilling new productive wells should be along central part of the studied area.

4.2.2. Lateral distribution of shale content

The lateral variation of shale content in main pay reservoirs in the studied area (Fig. 10a) shows that the high shale percentage gradient at the south eastern and south western part of the studied area at AM-16 and AM-7 wells and the minimum shale content at the middle northern and middle southern part of the studied area at AM-19 and AM-13 wells. The shale content of total pay zones (Fig. 10b) demonstrates that the shale content increases to be over

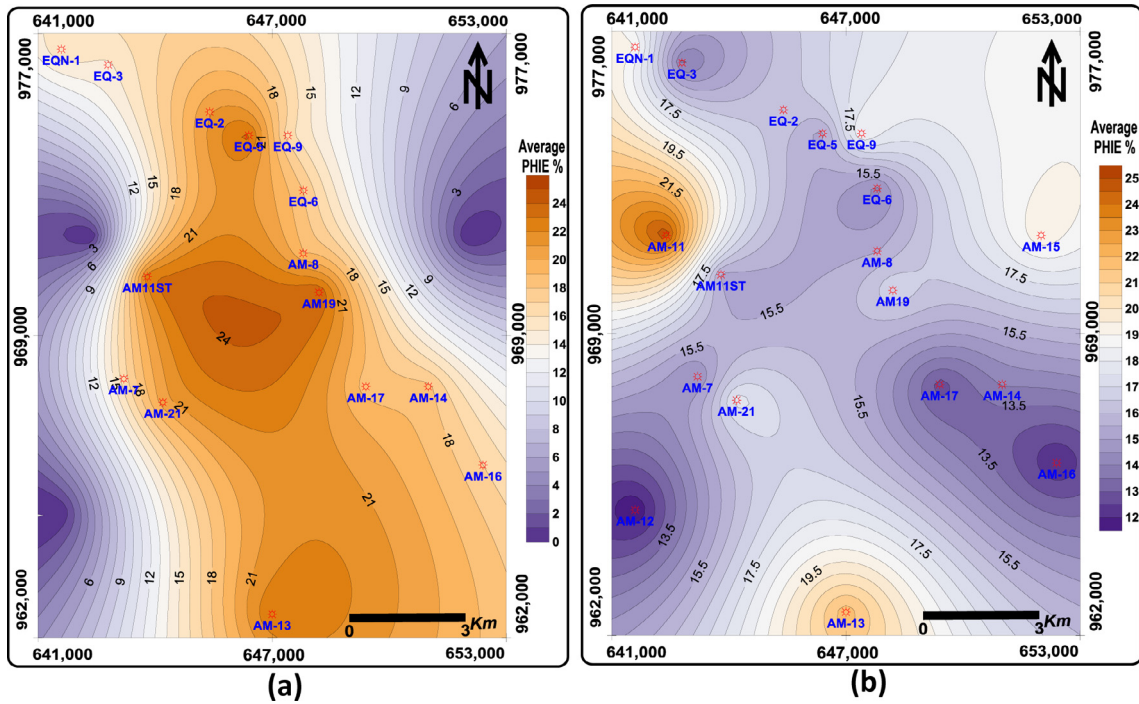


Fig. 11. Average effective porosity distribution map of (a) main pay zone and (b) total pay zones.

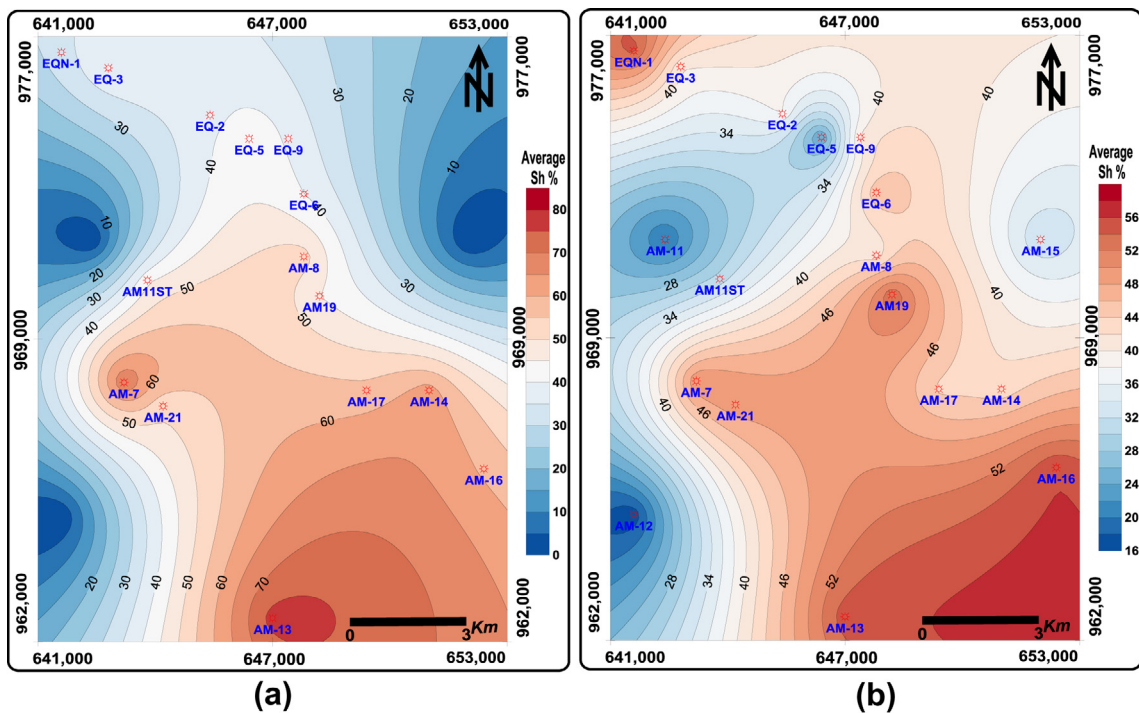


Fig. 12. Average hydrocarbon saturation distribution map of (a) main pay zone and (b) total pay zones.

45% at AM- well 5 in the southeast of the studied area; it decreases to less than 15% at AM-7, AM-11, AM-11ST, and EQ-5 wells in the north western part of the studied area.

4.2.3. Average effective porosity distribution map

The effective porosity distribution map for main pay reservoirs (Fig. 11a) reveals that the lateral variation in porosity values from lowest value at AM-7, AM-16, EQ-3 and EQN-1 wells in central

west, south east and north west part of the study area respectively. The middle, and central southern parts of the studied area are higher in average porosity in both lower and upper parts of Abu Madi Formation. The effective porosity map of the total pay zones (Fig. 11b) indicates that the porosity reaches its highest value of 24.95% at AM-11 well, and the minimum of 5.27% at AM-5 well in the southeastern part of the studied area; the northern and middle parts of the study area are higher in average porosity. The

effective porosity increases along the direction where shale volume decreases and main pay thickness increase.

4.2.4. Hydrocarbon saturation distribution map

The hydrocarbon saturation contour map of the lower and upper Abu Madi reservoirs (main pay) (Fig. 12a) shows that the high hydrocarbon saturation values over 60% are located toward the southern area at AM-13, AM-16 and AM-7 wells. The northern part of the studied area is characterized by low hydrocarbon saturation. In general, the hydrocarbon saturation of the studied area increased from south to north. The hydrocarbon saturation map of the total pay zones (Fig. 12b) shows a decrease toward the west to reach 16.60% at well AM-12 and 18.90% at well AM-5 respectively. The favorable area for gas accumulation is located at south and central parts of the studied area.

5. Conclusion

The geological information and the petrophysical parameters results from well logging analysis of Abu Madi Formation in both Abu Madi and El Qar'a fields, give good information about the lithology and the hydrocarbon prospect of the Late Miocene Abu Madi Formation in the studied area. From the cross –plot analysis we concluded that the lithological description of the reservoirs in both lower and upper parts of Abu Madi Formation composed of thick porous sandstone with some shale intercalations. Conversely, the upper part of Abu Madi Formation are composed of shale with sandstone intercalations in most wells. The cross-plot of the clay type was useful for detecting the environment of deposition of Abu Madi Formation which has been deposited in fluvial to shallow

marine environments. The weighted average contour maps for parameters such as effective thickness, average shale volume, average porosity and hydrocarbon saturations were illustrating that lower and upper parts of Abu Madi Formation in the studied area have promising reservoirs characteristics in which the prospective area for gas accumulation are located toward the south and central part of the area.

References

- [1] S. Dalla, H. Harby, M. Serazzi, Hydrocarbon exploration in a complex incised valley fill: an example from the late Messinian Abu Madi Formation (Nile Delta Basin, Egypt), *Lead. Edge* 16 (12) (1997) 1819–1824.
- [2] A. Rizzini, F. Vezzani, V. Cococetta, G. Milad, Stratigraphy and sedimentation of a Neogene–Quaternary section in the Nile Delta area, *Mar. Geol.* 27 (1978) 327–348.
- [3] M. Douglas, Exploration Potential for the Abu Madi Fm. And the Identification of the Fm. Boundaries for the Abu Madi, Qawasim and Sidi Salem Formations. Calgary: Centurion Energy International Inc, 2007.
- [4] M. Sarhan, K. Hemdan, North Nile Delta structural setting and trapping mechanism, 12th Petroleum Exp. & Prod. Conf., 1 (1994) 18.
- [5] I. El-Heiny, N. Enani, Regional stratigraphic interpretation pattern of Neogene's sediments, Northern Nile Delta, Egypt, in Proceedings of the 13th EGPC, Exploration and Production Conference, Cairo, Egypt (1996).
- [6] M. Alfay, F. Polo, M. Shash, The geology of Abu Madi Gas Field, in Proceedings of the 11th Petroleum Exploration and Production Conference, EPGC, Cairo, 1992, 485–513.
- [7] F. Tarek Shazly, Wafaa Abd Elaziz, Petrophysical evaluation of the Upper Cretaceous section in Abu Rudeis-Sidri Area, Gulf of Suez, Egypt using well logging data, *J. Appl. Geophys.* 7 (2010) 1–14.
- [8] A.A El Khadragey, T.F. Shazly, M. Ramadan, M.Z El-Sawy, Petrophysical investigation to both Rudeis and Kareem formation, Ras Ghara oil field-Gulf of Suez, Egypt, *Egypt. J. Petrol.* 26 (2017), <http://dx.doi.org/10.1016/j.ejpe.2016.04.005>, in press.
- [9] A. Poupon, J. Leveaux, Evaluation of water saturations in Shaly formations, *Log Anal.* 12 (1971).